Laser induced modification of vanadate glasses

Ben Franta,[1] *Tim Williams,*[2] *Cory Faris,*[1] *Steve Feller*[1] *& Mario Affatigato**[,1]

[1] *Physics Department, Coe College, 1220 First Av. NE, Cedar Rapids, IA 52402, USA*
[2] *JASCO International Co., 4-21 Sennin-cho 2-chome, Hachioji, Tokyo 193-0835, Japan*

Manuscript received 4 December 2006
Revised version received 3 July 2007
Accepted 13 July 2007

We report on our investigation of the effects of 785 nm light irradiation on lead vanadate glasses. Whereas high powers (>84 mW) yielded crystallisation and thermal modification of the surface, low powers (<38 mW) altered the sample without causing crystal formation. Scanning probe microscopy and micro-Raman spectroscopy were used to characterise the changes induced by the laser light. As part of the work we made glasses in the range 10 <x<60, where x is the molar percent of lead oxide, as well as crystals corresponding to $2PbO.V_2O_5$, $3PbO.V_2O_5$, and $8PbO.V_2O_5$. We also looked at the crystallisation of other binary vanadate glass families. The healing of low power damaged areas by annealing was studied, and we also made calorimetric measurements on the glasses.

I. Introduction

The crystallisation of glasses upon irradiation with a laser light source has been known and studied for several years. Cesium metaborate glasses have been crystallised[(1)] using 488 nm light, at powers of 600 mW, and the recrystallisation of $GeSe_2$ has also been investigated.[(2)] More recently,[(3)] 244 nm ultraviolet light was used to crystallise zinc tellurite and PbI_2-doped lead germanate glasses, and spatially selective patterning of borates was also shown[(4)] with a Nd:YAG laser. Lead vanadate glasses have been well characterised over the past three decades, though new, rapidly cooled families are still being investigated. Interest in these glasses arises from their semiconducting character, and some controversy[(5–7)] regarding their structure.

We report on our studies of the laser irradiation of vanadate glasses, especially lead vanadates, that can be crystallised with 785 nm light at relatively low (~84 mW) powers. We also investigated other changes to the glass surface that occurred upon exposure to lower laser powers and the healing of these damaged areas by annealing. Finally, we carried out a series of thermal measurements to determine the glass transition and crystallisation temperatures, as well as the specific heat of the glass samples.

II. Experimental procedure

A. Glassmaking procedure

Glasses were prepared according to the stoichiometry

$$x\mathrm{PbO}+(1-x)\mathrm{V_2O_5}\rightarrow x\mathrm{PbO}.(1-x)\mathrm{V_2O_5} \quad (1)$$

The starting materials for the glasses were lead (II) oxide (Aldrich, 99·9%), and vanadium (V) oxide (Aldrich, 99·6%). Lead vanadate glasses with stoichiometries ranging from $10PbO.90V_2O_5$ to $60PbO.40V_2O_5$ were prepared (Table 1). The powders were thoroughly mixed in a platinum crucible and heated to 1000°C in an electric muffle furnace. After 10 min the melt was removed from the furnace, let cool, and a weight measurement taken to ensure composition. The sample was placed back in the furnace for a further 10 min at 1000°C and subsequently cooled by splat quenching between two stainless steel plates. The cooling rate was approximately 10 000°C/s. Sample thickness was approximately 1·5 mm. Other vanadate glasses were also made, starting with oxides of sodium, bismuth, calcium, and magnesium, and prepared under similar conditions.

Glass transition (T_g) and crystallisation temperatures (T_x) were measured with a Perkin-Elmer DSC-7. As in our previous work, thermal scans were performed at 40°C/min and the onset definition of the T_g and T_x was used. The estimate for experimental error in calculating the T_g is ±5°C. To determine the specific heat, we subtracted the baseline heat flow curve from that of the sample and encapsulating pan. Following the manufacturer's instructions, the value of the heat flow difference ΔY at a point in the stable range 60–90°C was taken, and used to calculate the specific heat C_p using

$$C_p = \frac{\Delta Y}{m\beta} \quad (2)$$

where m is the mass of the sample and β is the heating rate of 40°C/min. By running a few references such as indium and gold we estimate the error to be on the order of 2%.

[1] Corresponding author. Email MAFFATIG@coe.edu

B. Laser irradiation procedure

The Raman system used for the laser irradiation (and analysis) was a JASCO NRS-3100 micro-Raman spectrophotometer. A Torsana Starbright 785 nm SLM diode laser was used to irradiate the sample at various power settings (16 mW, 41 mW, 84 mW, and 160 mW) for durations ranging from 5–20 s. A 532 nm Nd:YAG laser (maximum power of 5 mW, spot size approximately 1 μm) was also used. Spectra were then acquired at 1·7 mW at various sites in the resulting affected area; this power level was not enough to cause surface alterations. These were compared to spectra obtained from known crystalline compounds.

After being thoroughly crystallised at 84 mW, Raman spectra were taken of all compositions. Variations in crystal structure due to composition were observed.

Areas exposed to laser light were also studied for radial variations in structure. Radially distinct features were identified visually and analysed using Raman microscopy. Patterns in crystal structure as a function of distance from the centre of the affected area were identified.

C. Crystal formation and sample annealing

Crystalline compounds used include V_2O_5 (Aldrich), Pb(II)O (Aldrich), $2PbO.V_2O_5$, $3PbO.V_2O_5$, and $8PbO.V_2O_5$. The crystals $2PbO.V_2O_5$, $3PbO.V_2O_5$, and $8PbO.V_2O_5$ were made by mixing correct proportions of Pb(II)O and V_2O_5 to form 8 g batches. After being made into glasses using the procedure above, each sample was devitrified by holding it at 460°C for at least 16 h. This temperature was above T_x but below the liquidus temperature for all of our samples. The final samples were clearly crystalline, but no checks on their phases were carried out.

The repair of exposed sites by annealing was investigated. Plate quenched $50PbO.50V_2O_5$ glass underwent laser exposure at 160 mW, 41 mW, and 16 mW for 10 s. The exposed samples were then annealed in the electric muffle furnace at temperatures ranging from 266°C to 305°C. Annealed samples were inspected under the optical microscope to look at the healing of exposed sites. Raman spectra were used to determine the structural nature of sites of interest.

D. Atomic force microscopy

Representative irradiated areas were also imaged using a Veeco Multimode Scanning Probe Microscope. The tapping atomic force mode was used, with a scanner mapping out 25 μm × 25 μm areas with a maximum z-range of 5·1 μm. The tips used were phosphorus-doped Si, with a resonance frequency in the range of 280 kHz. Other than the standard plane fitting algorithm, no other filters were applied.

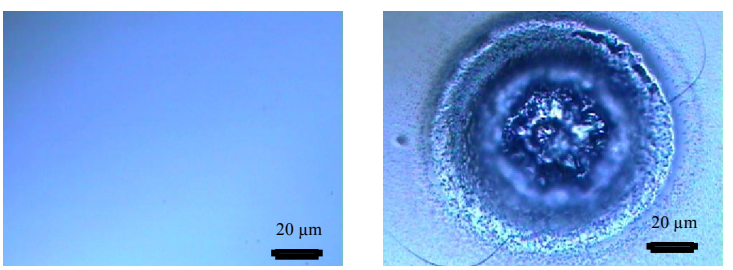

(a)

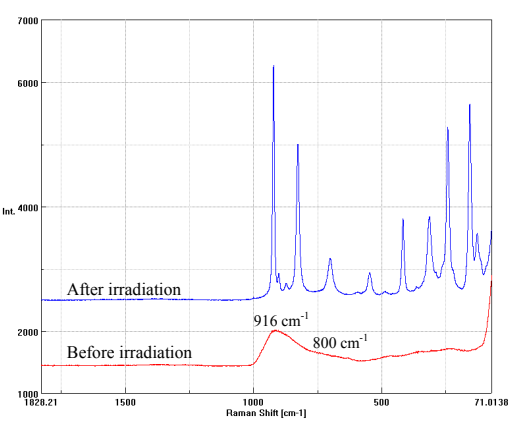

(b)

Figure 1. (a) Optical micrographs of a lead vanadate glass of composition $50PbO.50V_2O_5$, before irradiation (left) and after (right). The sample was irradiated at 100 mW for 10 s. (b) Raman spectra of the two locations, taken at very low powers. Note the crystallisation peaks

III. Results and discussion

The 785 nm results point to significant differences in the effects of the irradiation depending on the laser power used. High power (>84 mW, shown in Figure 1) yielded crystallisation of the exposed area, while low power (<38 mW) typically resulted in visible changes with a lack of crystal formation. Laser powers below 2 mW left the lead vanadate sample unaltered.

In general, the Raman band at 916 cm^{-1} is likely associated with the stretching vibrations of VO_3 units in metavanadate groups. The shoulder at 800 cm^{-1} has been linked[8,9] with a band arising from stretching modes of V–O–V bridges, attributed with pyrovanadate groups. Bands at lower (<500 cm^{-1}) frequencies are normally connected with lead oxide vibrations, but some vanadate minerals[10] have bands in the region 404–458 cm^{-1}.

High power irradiation

Figure 1 shows optical microscope images and Raman spectra of a $50PbO.50V_2O_5$ glass before and after laser irradiation with the 785 nm diode laser. Part (a) shows the obvious visible change in the surface. Given that the laser spot has a 1 μm diameter whereas the damaged area spans a diameter of 80 μm, it is quite likely that the changes are thermal in nature. The strong optical absorption of the glasses at the irradiation wavelength coupled to the low glass transition and crystallisation temperatures (see Table 1) results in laser induced thermodynamic changes even at modest power levels. The cracks observed at the periphery are also likely the results of thermal stress build up upon rapid heating. Figure 1(b) shows the Raman spectra obtained before and after the high power irradiation, and it displays the previously mentioned broad bands. The spectrum's multiple and sharpened peaks after irradiation point to a crystalline arrangement, confirming the optical microscope images.

Figure 2 shows the effect of the 10 s, 160 mW (full power) laser irradiation when analysed in the radial direction, starting from the centre, for a $50PbO.50V_2O_5$ glass. In Figure 2(a) we show an optical micrograph with three clearly delineated areas: a surface ridge near the centre pit (A); a concentric depression labelled (B); and another concentric region (C) at the same height as the original surface. The Raman spectra obtained from each of the three regions are shown in Figure 2(b), and clearly point to the formation of different crystal structures. We carried out a confocal Raman *z*-map of the region below the crystallised ridge. The strong optical absorption limited the usefulness of this technique, but the sample appears to have been crystallised to a depth of at least 60 μm below the ridge's surface.

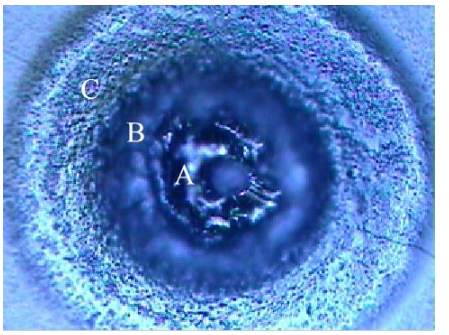

(a)

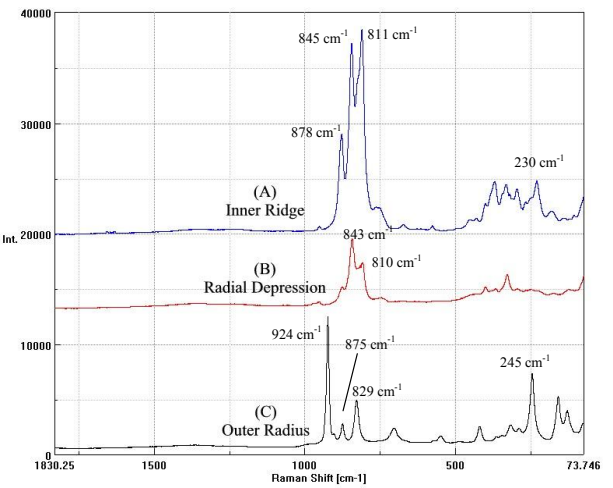

(b)

Figure 2. (a) Optical micrograph of a lead vanadate glass of composition $50PbO.50V_2O_5$, with different regions marked radially. (b) Raman spectra of the three radial locations A, B, and C. The glass was irradiated at 160 mW for 10 s at 785 nm, while the Raman spectra were taken with much lower powers (<2 mW)

Table 1. Calorimetric measurements on the lead vanadate glass system. The experimental errors are listed in the columns

Composition	T_g (°C, ±5°C)	T_x (°C, ±5°C)	C_p ($J\,kg^{-1}\,K^{-1}$), ±2%
$10PbO.90V_2O_5$	227	247	691
$20PbO.80V_2O_5$	235	259	639
$30PbO.70V_2O_5$	238	266	552
$40PbO.60V_2O_5$	245	289	501
$50PbO.50V_2O_5$	251	319	444
$60PbO.40V_2O_5$	262	293	410

The investigation of the crystallised region required an understanding of the possible crystal structures formed upon rapid heating of the sample. The phase diagram[12] of the binary $PbO–V_2O_5$ system shows three crystal structures at $2PbO.V_2O_5$, $3PbO.V_2O_5$, and $8PbO.V_2O_5$. By devitrifying glasses at the same compositions we were able to make all three crystals, and then characterise them using Raman spectroscopy. The lead metavanadate compound ($PbO.V_2O_5$) is also commercially available. Figure 3 illustrates the Raman spectra measured from the lead vanadate crystals as well as from the commercially

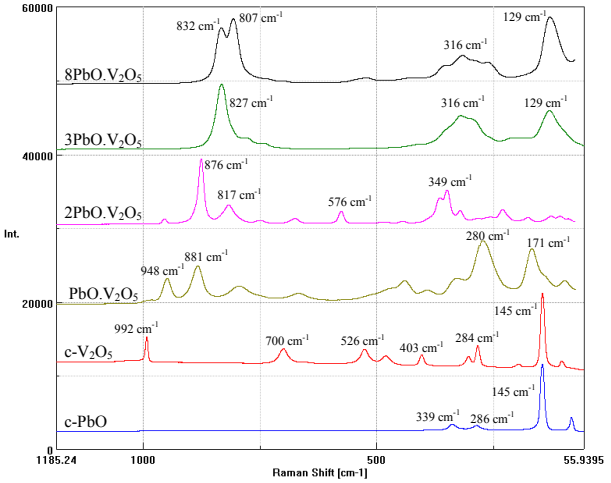

Figure 3. Collection of Raman spectra taken from a variety of crystalline compounds, including the starting oxides PbO and V_2O_5. The crystals $2PbO.V_2O_5$, $3PbO.V_2O_5$, and $8PbO.V_2O_5$ were obtained by devitrifying the glass samples; the lead metavanadate sample was commercial (Aldrich Chemical Co.)

obtained vanadium pentoxide, lead metavanadate, and lead monoxide. In Figure 4 we compare the Raman spectra attained from the outer radius and the inner ridge of Figure 2 to two of the crystal forms. In general, we observe that the inner ridge – closest to the centre and thus the laser spot – matches a crystal mix rich in the $8PbO.V_2O_5$ crystal, which is the one that forms at higher temperatures. The outer radius, on the other hand, is also a crystal mix, but composed of a blend richer in $2PbO.V_2O_5$. The presence of lead metavanadate cannot be ruled out, albeit in small amounts. This was contrary to our expectations, as we thought that the lead metavanadate crystal, similar in structure to the glass[5] in the form of

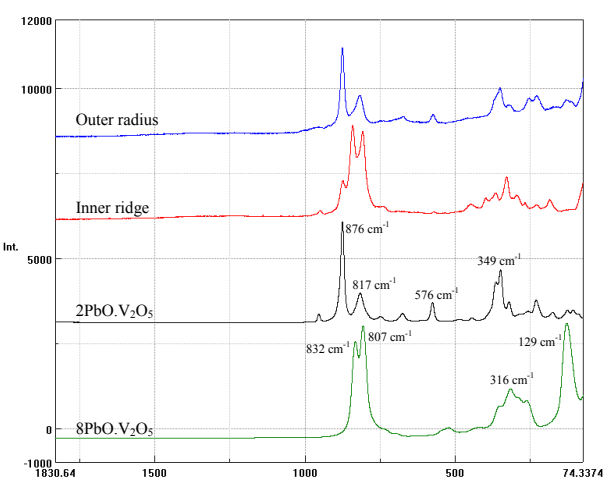

Figure 4. Comparison of the inner ridge (A) and the outer radius (C) to the crystals $2PbO.V_2O_5$ and $8PbO.V_2O_5$. The inner ridge shares some characteristics with a mix rich in $8PbO.V_2O_5$, while the outer radius has a blend richer in $2PbO.V_2O_5$

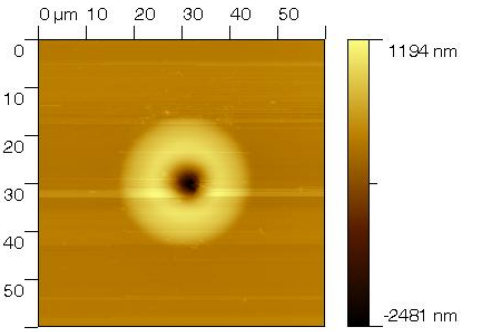

(a)

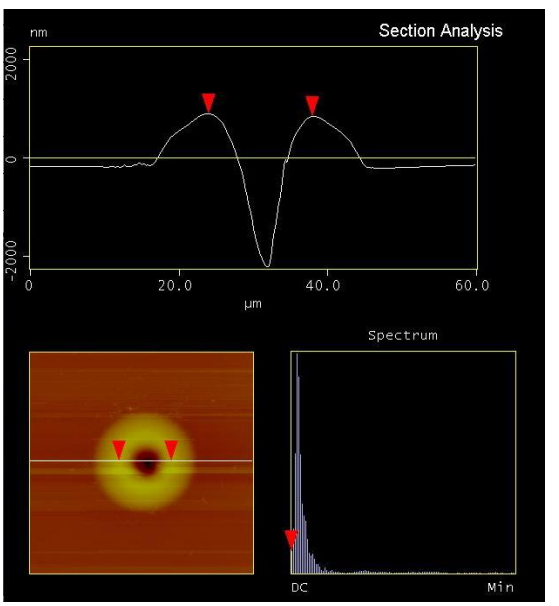

(b)

Figure 5. (a) Topview of an atomic force microscope image of a laser spot irradiated at 38 mW for 10 s. The sample was a $50PbO.50V_2O_5$ glass. (b) Cross sectional view of the altered area, indicating a rise (ridge) of approximately 1 µm above the original glass surface. The diameter of the damage spot is circa 30 µm

$(V_2O_8)_n$ chains,[11,13] would be the natural end product after laser crystallisation. The overall result can be explained by a simple heat diffusion mechanism in which the area closest to the centre attains higher temperatures and can form the corresponding crystal structures, while the outside region is cooler (though likely molten during irradiation) and does not behave in the same manner.

Low power irradiation

Figure 5 (a) and (b) shows an atomic force microscope image of a spot irradiated at low power, including a diametrical cross section (b). The spot did not show any crystallisation, but the cross section illustrates that the surface underwent drastic changes. A ridge

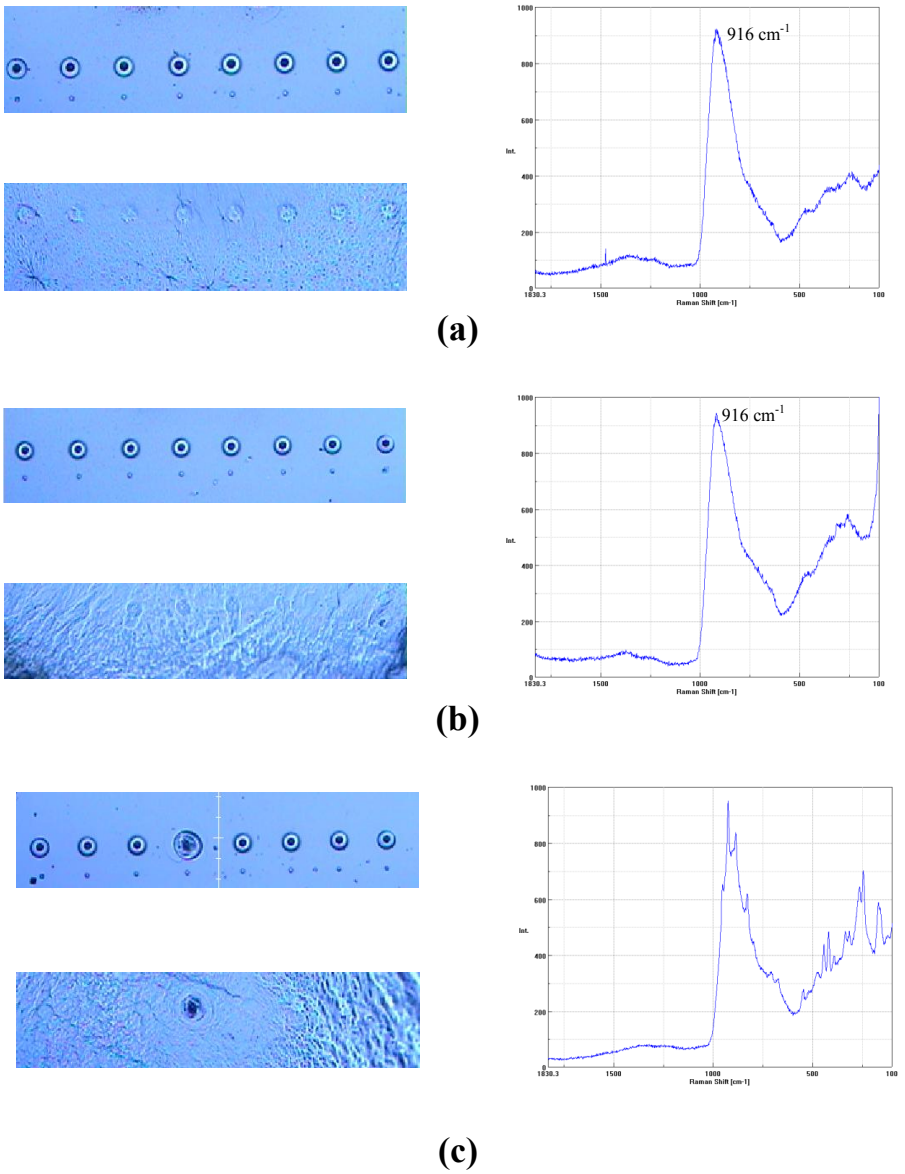

Figure 6. Effect of annealing on the altered spots of a 50PbO.50V_2O_5 glass. The initial irradiation, carried out at 16 mW for 10 s, did not lead to crystallisation in the spots. (a), (b), and (c) show the effect of annealing at 285°C after 2, 4, and 6 h, respectively. On the left are optical micrographs, showing before annealing (top), and after (bottom). On the right are Raman spectra taken on areas not irradiated by the laser light

again encircles a central pit, suggesting a thermally driven melting and resolidification. The pit's apparent depth is only 2 μm, but this is likely an artefact: the cantilever of the scanning probe microscope cannot explore the true depth of the hole. The area visibly affected is approximately 15 μm across (radius), much larger than the 1 μm laser spot diameter. The centre hole has a radius of 10 μm, comparable to micro-holes made[14] by femtosecond laser irradiation of fused silica.

Figure 6 shows optical microscope images (left) and Raman spectra (right) of an irradiated 50PbO.50V_2O_5 glass before and after annealing. The power used was not sufficient to crystallise, but only to cause surface changes. Figure 6(a) shows the results after annealing at 285°C for 2 h, while the samples in Figure 6(b) and (c) were annealed for 4 and 6 h at the same temperature, respectively. The temperature was chosen to be above the glass transition temperature (T_g) but below the crystallisation temperature (T_x) for this composition (see Table 1). The optical images illustrate a series of damage spots done at 38 mW (top row) and at 15 mW (bottom row). The Raman spectra on the right are of the area after the annealing. In general, the annealing at 2 and 4 h removed much of the damage while keeping the sample glassy. After 6 h there was evidence of crystalline growth across the entire surface. This last effect may have been enhanced by the formation of nucleation sites following laser irradiation, though the crystal growth

did not appear to start at the damaged spots. Hence, it may well be the results of homogeneous crystallisation in the glass itself, and unrelated to the laser irradiation.

Other vanadates

The mechanism of the laser induced crystallisation appears to be thermal in nature. As a check, we irradiated other glasses. After exposure at 1·26 mW with a 532 nm, Nd:YAG laser, for instance, we were able to crystallise both lead metavanadate glass ($PbO.V_2O_5$) and a sodium vanadate glass sample of composition $0{\cdot}2Na_2O.0{\cdot}8V_2O_5$. After a 30 s exposure at 2·5 mW, bismuth vanadate glass ($0{\cdot}05Bi_2O_3.0{\cdot}95V_2O_5$) was also crystallised. And calcium vanadate ($0{\cdot}41CaO.0{\cdot}59V_2O_5$) crystallised after 30 s at 4·6 mW. Magnesium vanadate glass ($0{\cdot}33MgO.V_2O_5$), on the other hand, could not be crystallised even at the highest available Nd:YAG power of 5 mW. We attributed this to the sample's higher glass transition and crystallisation temperatures (306°C and 369°C, respectively). From Table 1 we can also note that the specific heat of the glasses decreases as the lead content is increased, which correlates well with the growing ease of crystallisation. The effect allows the same laser power to attain higher temperatures in the sample for higher lead concentrations. Thus, the combination of strong optical absorption and low glass transitions and melting points makes this family of glasses especially suitable for laser induced thermal transformations.

IV. Conclusions

We have investigated changes in the morphology of the surface of lead vanadate glass upon laser irradiation by 785 nm laser light. At low laser powers (<38 mW), the exposed areas are visibly altered, the result of thermally driven damage. Annealing at 285°C for 4 h was shown to reduce the damage substantially, leading to healing of the affected areas. Further annealing began to crystallise the surface of the sample.

At high laser powers (>84 mW), the irradiated areas showed the appearance of crystallisation. Polycrystalline zones appeared, differing in their crystal mix depending on their radial distance from the central laser irradiation spot. Contrary to expectations, lead metavanadate was not the dominant crystal structure present, perhaps because of changes in its structure at more elevated temperatures. The structural change could not be reversed.

Measurements of the specific heat (C_p) of the glass samples fall in the range of values between our measured values for lead oxide (211 J/(kg °C)) and vanadium pentoxide (756 J/(kg °C)). The steady increase in the C_p results in easier crystallisation as the lead content is increased.

V. Acknowledgments

This research was supported by the National Science Foundation under grant DMR-CER-0502051. Other financial support was received by the Roy J. Carver Charitable Trust of Iowa in the form of the Carver Scholars program. Mr M. Vu is also thanked for aid in the scanning of some samples, and Mr J. Borden's help with the Raman spectrometer is gratefully acknowledged.

References

1. Kamitsos, E. I., Karakassides, M. A., Patsis, A. P. & Chryssikos, G. D. *J. Non Cryst. Solids*, 1990, **116**, 115–122.
2. Haro, E., Xu, Z. S., Morhange, J. F., Balkanski, M., Espinosa, G. P. & Phillips, J. C. *Phys. Rev. B*, 1985, **32**, 969–979.
3. Goutaland, F., Mortier, F., Capoen, B., Turrell, S., Bouazaoui, M., Boukenter, A. & Ouerdane, Y. *Opt. Mater.*, 2006, **28**, 1276–1279.
4. Honma, T., Benino, Y., Fujiwara, T., Sato, R. & Komatsu, T. *J. Non Cryst. Solids*, 2004, **345&346**, 127–131.
5. Hayakawa, S., Yoko, T. & Sakka, S. *J. Non Cryst. Solids*, 1995, **183**, 73–84.
6. Mekki, A., Khattak, G. D. & Wenger, L. E. *J. Non Cryst. Solids*, 2003, **330**, 156–167.
7. Hoppe, U., Kranold, R., Ghosh, A., Landron, C., Neuefeind, J. & Jovari, P. *J. Non Cryst. Solids*, 2003, **328**, 146–156.
8. Maniu, D., Iliescu, T. & Astilean, S. *Romanian Reports*, 2004, **56**, 419–423.
9. Lewandowska, R., Krasowski, K., Bacewicz, R. & Garbarczyk, J. E. *Solid State Ionics*, 1999, **119**, 229–234.
10. "Raman Spectroscopy of Selected Vanadates", Carmody, O., Wier, M. & Frost, R. *Proc. XIX International Conference on Raman Spectroscopy*, in http://www.publish.csiro.au/issue/1051.htm, (Csiro Publishing), 2004.
11. Hayakawa, S., Yoko, T. & Sakka, S. *Bull. Chem. Soc. Jpn.*, 1993, **66**, 3393–3400.
12. *Phase Diagrams for Ceramists, Vol. I*, Eds E. M. Levin, C. R. Robbins & H. F. McMurdie, American Ceramic Society, Columbus, OH, 1985, Fig. 290.
13. Hayakawa, S., Yoko, T. & Sakka, S. *J. Solid State Chem.*, 1994, **112**, 329–339.
14. Kasaai, M. R., Lagace, S., Boudreau, D., Forster, E., Muller, B. & Chin, S. L. *J. Non Cryst. Solids*, 2001, **292**, 202–209.